Long-distance electron transport in individual, living cable bacteria

Jesper T. Bjerg[a,b,1], Henricus T. S. Boschker[c,d], Steffen Larsen[b], David Berry[e,f], Markus Schmid[e,f], Diego Millo[g], Paula Tataru[h], Filip J. R. Meysman[d,c], Michael Wagner[e,f], Lars Peter Nielsen[a,b], and Andreas Schramm[a,b,1]

[a]Center for Electromicrobiology, Aarhus University, DK-8000 Aarhus C, Denmark; [b]Center for Geomicrobiology, Section for Microbiology, Department of Bioscience, Aarhus University, DK-8000 Aarhus C, Denmark; [c]Department of Biotechnology, Delft University of Technology, 2629 HZ Delft, The Netherlands; [d]Ecosystem Management Research Group, Department of Biology, University of Antwerp, BE- 2610 Wilrijk, Belgium; [e]Division of Microbial Ecology, Department of Microbiology and Ecosystem Science, University of Vienna, A-1090 Vienna, Austria; [f]Research Network Chemistry Meets Microbiology, University of Vienna, A-1090 Vienna, Austria; [g]Department of Physics and Astronomy, Vrije Universiteit Amsterdam, 1081 HV Amsterdam, The Netherlands; and [h]Bioinformatics Research Centre, Aarhus University, DK-8000 Aarhus C, Denmark

Edited by Edward F. DeLong, University of Hawaii at Manoa, Honolulu, HI, and approved April 3, 2018 (received for review January 8, 2018)

Electron transport within living cells is essential for energy conservation in all respiring and photosynthetic organisms. While a few bacteria transport electrons over micrometer distances to their surroundings, filaments of cable bacteria are hypothesized to conduct electric currents over centimeter distances. We used resonance Raman microscopy to analyze cytochrome redox states in living cable bacteria. Cable-bacteria filaments were placed in microscope chambers with sulfide as electron source and oxygen as electron sink at opposite ends. Along individual filaments a gradient in cytochrome redox potential was detected, which immediately broke down upon removal of oxygen or laser cutting of the filaments. Without access to oxygen, a rapid shift toward more reduced cytochromes was observed, as electrons were no longer drained from the filament but accumulated in the cellular cytochromes. These results provide direct evidence for long-distance electron transport in living multicellular bacteria.

cable bacteria | Raman spectroscopy | cytochrome c | conduction | electromicrobiology

Cable bacteria are multicellular, centimeter-long filamentous bacteria that occur globally in marine and freshwater sediments (1–5). In their presence the sediment exhibits an electrical coupling between the oxidation of sulfide (H_2S) in deeper sediment layers and the reduction of oxygen (O_2) near the sediment–water interface, thereby generating a 1–4-cm-deep suboxic zone devoid of O_2 and H_2S (6, 7). Cable bacteria spanning this suboxic zone thus appear to transfer electrons over centimeter distances, which is several orders of magnitude longer than previously found in any organism (1, 7–10). Long-distance electron transport by cable bacteria is supported by several observations: (*i*) changes in oxygen availability in the water column have an immediate effect on sulfide oxidation several centimeters into the sediment, which is faster than what can be explained by diffusion (6); (*ii*) electron transport occurs even where cable bacteria span a nonconductive barrier in the sediment like an inserted glass bead layer or a filter with pore size ≥2 μm (1); and (*iii*) a wire cutting through the suboxic zone rapidly disrupts conduction (1). However, direct demonstration of electric conductance by individual cable-bacteria filaments is still lacking (1, 11).

The mechanism of conductance has remained unclear but continuous periplasmic fibers, running along the entire filament length, have been proposed as conducting elements (1). Electrostatic force microscopy measurements indicated a significant charge-storage capacity in these fibers (1). Capacitance has also been observed in another electrogenic bacterium, *Geobacter sulfurreducens*, where it is due to abundant c-type cytochromes (12). The type and redox state of cytochromes can be analyzed using resonance Raman microscopy (13), and this method has revealed gradients in cytochrome redox states in electrically conductive *Geobacter* biofilms (14–16). We hypothesized that any electron conduction by the cable bacteria from sulfide to oxygen must be associated with a potential gradient along the conductive structure (7). Since cytochromes are common electron carriers in bacterial cells, we further hypothesized that, as seen in *Geobacter* biofilms, this potential gradient should be reflected by the redox state of cytochromes. Here we used resonance Raman microscopy as a noninvasive technique to detect a gradient in cytochrome redox state along living cable-bacteria filaments and to demonstrate its dependence on an intact electrical connection between the electron donor H_2S and the electron acceptor O_2.

Results

Positioning of Living Cable Bacteria in Gradients of Sulfide and Oxygen. We constructed a microscope chamber setup (Fig. S1) that allowed us to position individual cable-bacteria filaments between a sulfide source and an oxygen source located 5 mm apart from each other (17) (see *SI Methods* for details). Sediments from one freshwater site and two marine sites were enriched for cable bacteria (*SI Methods*) and used as source of sulfide and cable bacteria. Within a day, cable bacteria emerged from the sediment and reached the oxic zone near the air inlet (Movie S1 and ref. 17). Cable-bacteria filaments, which had emerged from the sulfidic sediment but had not yet reached the oxic zone, were used as controls. Swarming, microaerophilic

Significance

Cable bacteria are centimeter-long, multicellular filamentous bacteria, which are globally occurring in marine and freshwater sediments. Their presence coincides with the occurrence of electrical fields, and gradients of oxygen and sulfide that are best explained by electron transport from sulfide to oxygen along the cable-bacteria filaments, implying electric conductance by living bacteria over centimeter distances. Until now, all indications for such long-distance electron transport were derived from bulk sediment incubations. Here we present measurements on individual cable-bacteria filaments that allow us to quantify a voltage drop along cable-bacteria filaments and show a transport of electrons over several millimeters. This is orders of magnitude longer than previously known for biological electron transport.

Author contributions: J.T.B., H.T.S.B., S.L., F.J.R.M., M.W., L.P.N., and A.S. designed research; J.T.B., H.T.S.B., S.L., M.S., and D.M. performed research; J.T.B., D.B., D.M., P.T., and L.P.N. analyzed data; and J.T.B., H.T.S.B., and A.S. wrote the paper.

The authors declare no conflict of interest.

This article is a PNAS Direct Submission.

See Commentary on page 5632.

[1]To whom correspondence may be addressed. Email: jjbjerg@bios.au.dk or andreas.schramm@bios.au.dk.

This article contains supporting information online at www.pnas.org/lookup/suppl/doi:10.1073/pnas.1800367115/-/DCSupplemental.

Published online May 7, 2018.

single-celled bacteria positioned themselves approximately 1 mm from the air inlet (Fig. 1*A*), and microsensor measurements showed that this bacterial veil provided a good marker for the oxic–anoxic transition zone. Microsensor measurements further confirmed the absence of sulfide and oxygen in a 4-mm-wide suboxic zone between the veil and the sediment edge (Fig. 1*B*).

Resonance Raman Microscopy Reveals c-Type Cytochromes in Cable Bacteria. We recorded nearly 2,000 Raman spectra for 15 cable-bacteria filaments, which spanned the suboxic zone from sulfide to oxygen. Cable-bacteria diameters ranged from 1.6 to 6.6 μm, and only motile filaments were used, as these are certain to be metabolically active. All filaments displayed the four most prominent bands reported for c-type cytochromes at 750 (ν_{15} pyrrole breathing mode), 1,130 (ν_{22}), 1,315 (ν_{21}), and 1,588 cm^{-1} (ν_2) (Fig. 2*A* and Figs. S2 and S3) (17), which all decreased in intensity across the suboxic zone from near the sediment to the oxygen front. Thick filaments (>4-μm diameter) provided more detailed spectra, with additional small bands of several vibrational modes of the cytochrome heme groups (Fig. 2*A* and Fig. S2). Near the sediment, the ν_4 and ν_3 bands were centered at 1,361 and 1,496 cm^{-1}, respectively (Fig. 2*A* and Fig. S2, red trace). Near the oxic zone, the overall spectra intensity decreased, the ν_4 band shifted to 1,369 cm^{-1}, the ν_3 band was no longer detectable, and a broad ν_{10} mode at 1,637 cm^{-1} appeared (Fig. 2 *A* and *B*, and Fig. S2, blue trace). All these changes are consistent with a c-type heme having a six-coordinated low-spin central iron atom varying its oxidation state from reduced (near the sediment) to oxidized (near oxygen) (18, 19). Broadening of the ν_2 (featuring a shoulder at 1,593 cm^{-1}) and ν_{10} bands suggests the presence of at least two different conformers having His-Fe-His and His-Fe-Met axial ligation (18). Both of these conformers were also detected for *Geobacter* species grown on electrodes, where these cytochromes connect the cell metabolism to the electrode (13, 20).

Cytochrome Redox State Changes Gradually Along the Cable-Bacterium Filaments. Throughout the rest of the study, the most prominent band in all cable-bacteria filaments, at 750 cm^{-1} (Fig. 2*A* and Fig. S3), was used as proxy of cytochrome redox state (21, 22). Along all cable-bacterium filaments connected to both O_2 and H_2S (n = 15), we observed a gradual decrease of the absolute intensity of this 750-cm^{-1} band from the sulfidic sediment toward the oxic zone (Fig. 2 *B* and *C* and Fig. S4). In the subset of thick filaments (n = 6), we also observed a gradual increase of the band at 1,637 cm^{-1}. In contrast, filaments without connection to oxygen (n = 3) showed highly reduced spectra (n = 300) with high intensities of the 750-cm^{-1} band, even close to the oxic–anoxic transition. Filaments briefly incubated in oxic water (n = 4) all showed spectra typical for oxidized cytochromes (n = 98), with low intensities at 750 cm^{-1} (Fig. S5). These controls demonstrate that the observed differences in cytochrome band intensities along cable-bacteria filaments were not due to varying cytochrome abundance along the filaments, but are caused by the cytochrome redox state.

Fast Shift in Cytochrome Redox State upon Disconnection of O_2. To directly link the change in cytochrome redox state to electron transport along individual bacterial cables, we used two experimental manipulations that have previously been demonstrated to impede the electron flow in sediment cores with cable-bacteria activity (1, 6).

First, we removed oxygen from the air inlet by either filling the inlet with oxygen-free water or by flushing it with dinitrogen gas (Fig. 3*A*). Within approximately 10 min, the cytochrome redox state near the sediment, i.e., 4 mm away from the site of manipulation, showed a small but significant shift toward a more reduced pattern (Fig. 3*B*). This shift was more pronounced at the center of the suboxic zone (midpoint; Fig. 3 *A* and *B*), where the initial cytochrome redox state was more oxidized, in concordance with the redox potential gradient from sediment to oxic zone (Fig. 2*C*). The shift could be reversed by reintroducing oxygen, which reestablished the original redox state within 3 min, i.e., as fast as we could measure (Fig. 3*C*). Cable-bacteria filaments connected to the sediment but not to the oxic zone (Fig. 3*A*) had already highly reduced cytochromes and showed no change upon removal of oxygen.

In a second experiment, we stopped the electron transport by cutting individual filaments using a laser microdissection microscope and measured the response in cytochrome redox state

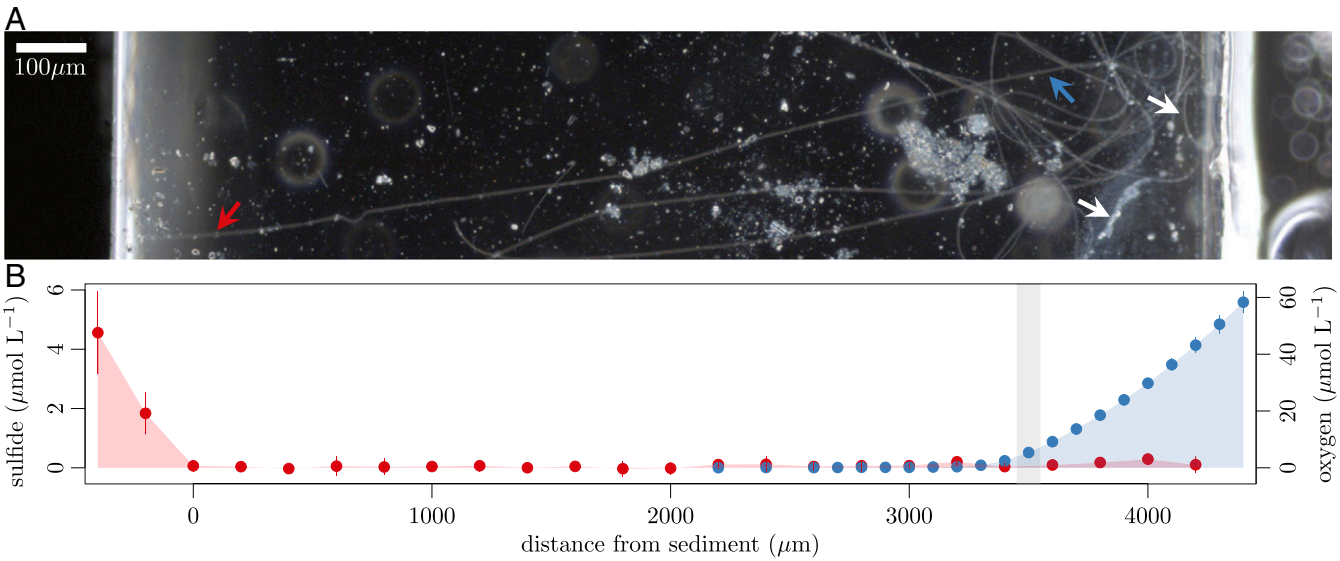

Fig. 1. (*A*) Dark-field micrograph of cable bacteria in the microscopic chamber setup reaching from sulfidic sediment (*Left*) to oxygen (*Right*). Arrows show the position of the veil composed of swarming microaerophilic microbes (white) and the positions, where the reduced (red) and oxidized (blue) Raman spectra shown in Fig. 2*A* were recorded. (*B*) Sulfide (red) and oxygen (blue) concentration gradients across the chamber setup as determined by microsensor measurements (n = 6). Gray shading indicates the microaerophilic veil.

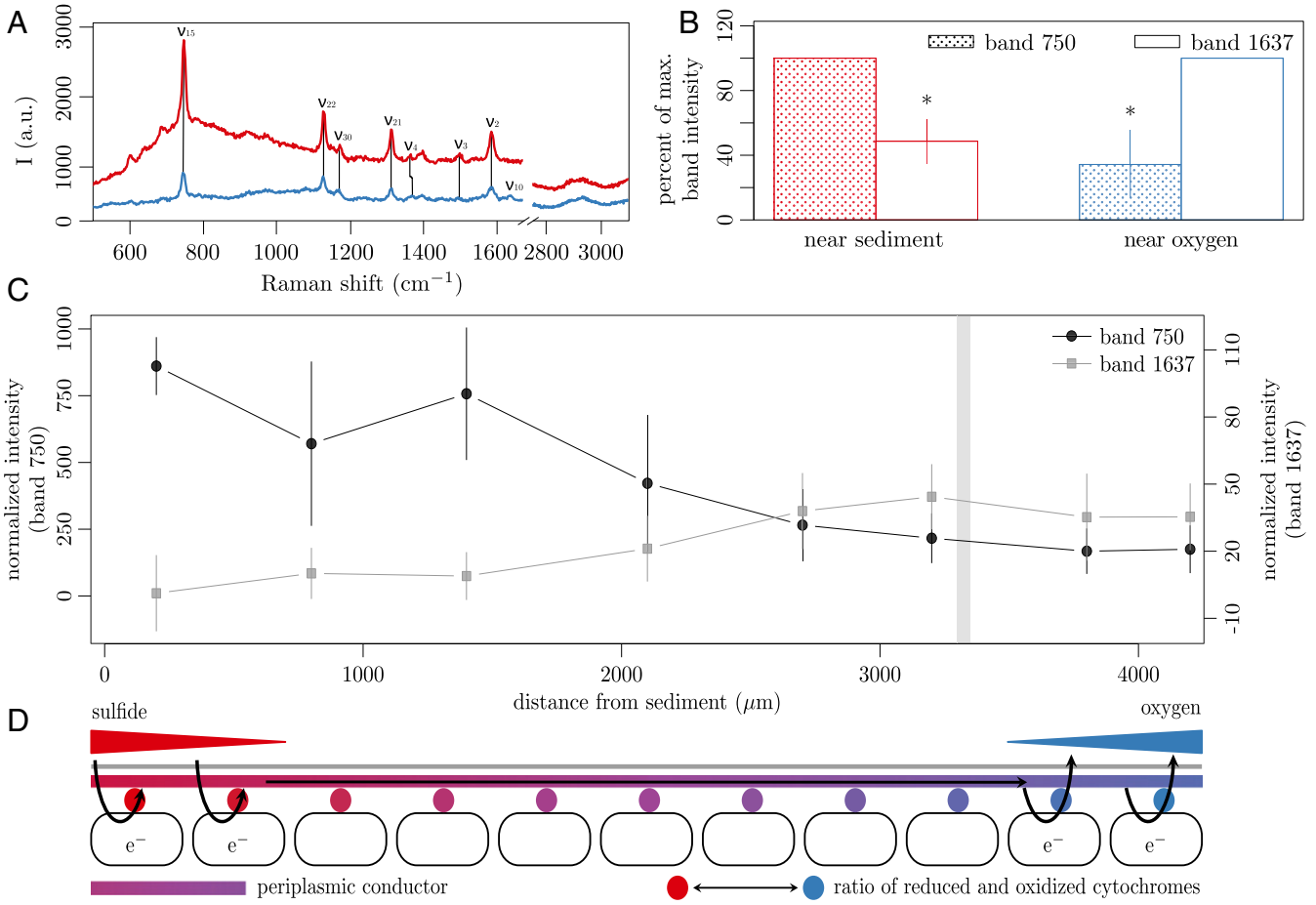

Fig. 2. (*A*) Raman spectra from an individual cable-bacterium filament (site Rattekaai, The Netherlands) near sediment (red) and near oxygen (blue). (*B*) Difference in normalized band intensity between either end of the suboxic zone. Red = data points closest to sediment (Fig. 1*F* and Fig. S4); blue = data points closest to microaerophilic veil and oxygen. Stippled and open bars display band intensities at 750 and 1,637 cm^{-1}, respectively, given as percentage of the maximum band intensities (mean ± SD). Asterisks depict significant differences between cable-bacteria ends. *n* (for 750-cm^{-1}/1,637-cm^{-1} band) = 15/6 filaments (379/200 spectra, Shapiro–Wilk test *P* value: 0.493/0.28, *t* test *P* value = 5.31×10^{-6}/8.8×10^{-4}). (*C*) Normalized band intensities (mean ± SD) showing the cytochrome redox gradient along a single cable-bacterium filament (Fig. S4*M*), reaching from sediment (to the left) toward oxygen. Gray shading indicates the microaerophilic veil. (*D*) Conceptual model of electron transport in cable bacteria. Cells in the sulfidic zone, with reduced cytochromes, upload electrons from H_2S to periplasmic fibers, while cells in the oxic zone, with oxidized cytochromes, download electrons from these fibers to O_2.

near the sediment edge (Fig. 4*A*). An advantage of this approach is that cutting a single filament will have only limited effects on sulfide and oxygen gradients. Within 5 min, a clear shift toward more reduced cytochromes was detected in the part of the cable filament that was still connected to the sediment (Fig. 4*B*). Cable bacteria not reaching the oxic zone showed no change in cytochrome redox state upon cutting.

Discussion

In both manipulation experiments, we observed a significant shift toward more reduced cytochromes when filaments were no longer connected to oxygen. With the terminal electron acceptor suddenly unavailable, cytochromes in the cable bacteria apparently accumulate electrons released by sulfide oxidation in the sediment and thereby become more reduced. The response time of minutes is too fast to be explained by diffusion of chemical compounds over a distance of millimeters either outside or inside the cable bacteria filaments. Therefore, we infer from our manipulation experiments that the rapid changes observed in the cytochrome redox state must depend on the capability of transporting electrons across millimeter distances from the sulfidic zone to the oxic zone.

At present, the exact role of the cytochromes in cable-bacteria–mediated electron transport from electron donor to electron acceptor remains elusive. The gradual change in cytochrome redox state cannot result from a change in the external redox conditions, as both oxygen and sulfide were absent from the intermediate, suboxic zone. The redox state of the cytochromes thus reflects an internal redox potential gradient within individual cable-bacteria filaments, which is consistent with three scenarios. First, the cytochromes could theoretically be part of the conductive structure, which would then suggest a mechanism of electron hopping via heme groups along the redox gradient (14, 23). However, the electron-hopping frequency and the amount of heme groups required to explain the observed rates of electron transport would be unprecedented (7). Secondly, cytochromes could operate in combination with pilus nanowires, as proposed for electroactive biofilms thicker than 10 μm (24). Finally, the cytochromes could be involved in the up- and downloading of electrons to and from a yet-unknown internal conductive structure (Fig. 1*D*). Analogous to how a voltmeter measures the electrical potential gradient along the length of a resistor, the cytochromes would then measure the potential gradient along the conductor. The observed gradient in

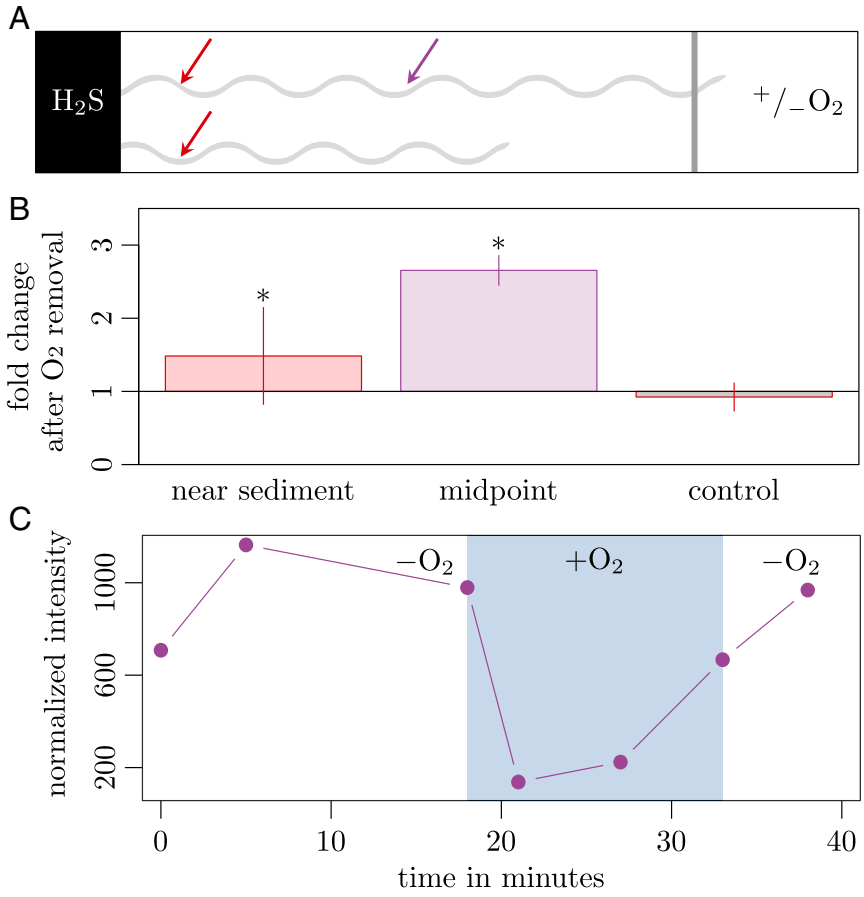

Fig. 3. Effect of oxygen availability on cable-bacteria redox state. (*A*) Schematic of the setup for oxygen manipulation experiments. A filament (light-gray wave) reaches out from sulfidic sediment (*Left*) toward the air inlet (*Right*), from which oxygen can be removed; dark-gray shading indicates the position of the microaerophilic veil. Filaments that did not reach the veil were used as controls. Positions of Raman spectra recordings are marked with red (near sediment) and purple (midpoint) arrows. (*B*) Change in cytochrome redox state resulting from a change in oxygen availability. Bars represent fold change in normalized band intensities at 750 cm^{-1} relative to the intensity in the presence of oxygen (mean ± SD). Significant changes in redox state are marked by an asterisk. $n = 16$ filaments near sediment (1,666 spectra, Shapiro–Wilk test *P* value: 0.0003, Wilcoxon sign test *P* value: 0.000122), $n = 4$ filaments at midpoint (50 spectra, Shapiro–Wilk test *P* value: 0.551, *t*-test *P* value: 0.000488), and $n = 6$ control filaments near sediment (744 spectra, Shapiro–Wilk test *P* value: 0.903, *t*-test *P* value: 0.659). (*C*) Change in cytochrome redox state (band intensity at 750 cm^{-1}) of a single cable-bacterium filament over time (42 min) during changes in oxygen availability. Measurements were done at midpoint. White area represents time when the air inlet was flushed with N_2; shaded blue area represents time with oxygen available.

cytochrome redox states thus reflects the voltage drop along the internal conductor of the cable bacteria.

This voltage drop can be quantified by applying the Nernst equation and the ratio of reduced to oxidized cytochromes at either side of the suboxic zone (for details see *SI Methods*). Using the cable-bacteria filaments with the largest diameters and thus the best-quality Raman spectra (Fig. S4 *I–O*), we calculated a voltage drop of 12.3–14.6 ± 3.8–4.1 mV mm^{-1} (mean ± SD; $n = 6$; Dataset S1). This voltage drop represents energy loss in the conductor. If extrapolated to the natural setting, where cable bacteria typically span suboxic zones of 20 mm, the voltage drop would be up to 293 mV to maintain the same current. Considering the theoretical maximum of about 1,000 mV available for aerobic sulfide oxidation, this is a significant dissipation of energy and it is suggested that extension of the operational length of a cable bacterium eventually forces a lower current or a lower energy yield per electron transferred.

These findings hence provide direct evidence of long-distance electron conduction in individual cable bacteria, which in our experiments takes place over several millimeters, i.e., about 1,000× the length of individual cells. In natural sediments, long-distance electron transport by cable bacteria is extended to centimeter distances (6).

Methods

Please see *Supporting Information* for a detailed description of the materials and methods.

Sampling and Incubation. Surface sediment was collected from a freshwater lake and two marine sites containing cable bacteria of the genera *Candidatus* Electronema and *Ca*. Electrothrix (4). The sediments were enriched in the laboratory for cable bacteria as previously described (1) and used for transfer to microscope chamber setups.

Microscope Chamber Setups. Two microscope chamber setups (Fig. S1) were used to examine cable-bacteria filaments. Both setups mimicked the redox gradient conditions that cable bacteria experience in their natural habitat, with a sulfide source (sediment) on one side, and an oxygen source (air) on the other side. In setup A, two wells (diameter 1–4 mm, separation 5 mm) were drilled into 4-mm-thick glass microscopy slides using a diamond drill. One well was filled with the cable-bacteria–enriched sediment, while the other was left open and hence filled with ambient air. Cable bacteria reached out of the sediment and moved across the water zone toward the air-filled well within 24 h (Movie S1).

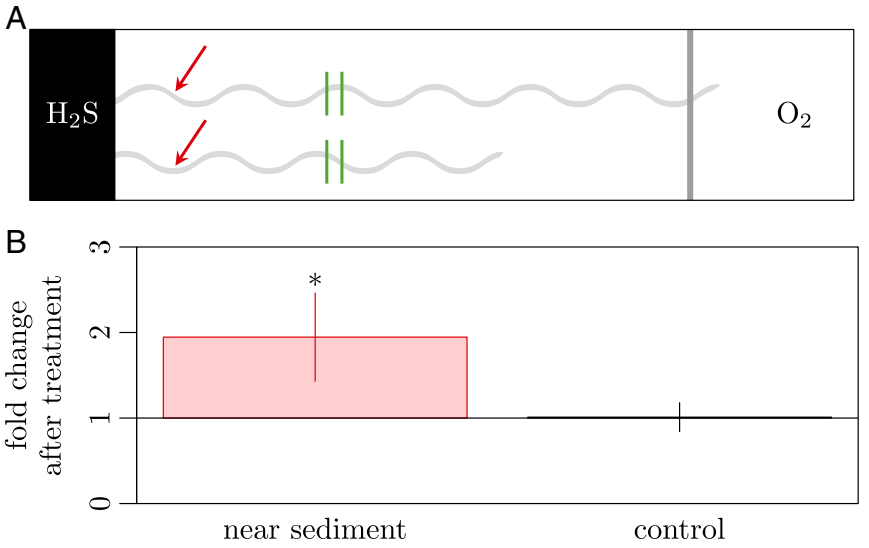

Fig. 4. Effect of filament cutting on cable-bacteria redox state. (*A*) Schematic of the setup for laser-cut experiments. A filament (light-gray wave) reaches out from sulfidic sediment (*Left*) toward the air inlet (*Right*); dark-gray shading indicates the position of the microaerophilic veil. Filaments that did not reach the veil were used as controls. Positions of Raman spectra recordings are marked with red arrows (near sediment), positions of laser cuts are marked with green bars. (*B*) Change in cytochrome redox state in response to laser cutting of the filaments. Bars represent fold change in normalized band intensities at 750 cm^{-1} relative to the intensity before the cut (mean ± SD). A significant change in redox state is marked by an asterisk. $n = 10$ filaments (1,143 spectra, Shapiro–Wilk test *P* value: 0.117, *t*-test *P* value: 0.000517) and $n = 5$ control filaments (852 spectra, Shapiro–Wilk test *P* value: 0.84, *t*-test *P* value: 0.879).

In setup B, glass slabs were glued onto a microscope slide, creating a trench in the middle, which was filled with the cable-bacteria–enriched sediment and covered with a coverslip. As in setup A, cable bacteria reached out of the sediment toward the oxic zone near the edge of the microscope slide.

Oxygen and Hydrogen Sulfide Microsensor Measurements. Microelectrodes for O_2 and H_2S were inserted between the microscope slide and the coverslip of slide setup B. O_2 and H_2S concentration were recorded from the edge of the coverslip until 2 mm into the suboxic zone, or all the way into the sediment, respectively.

Resonance Raman Microscopy. Raman spectra were recorded on confocal Raman microscopes (Horiba and Renishaw) along individual filaments of cable bacteria starting from the sediment and moving toward the air inlet. At each longitudinal position, 2–3 line scans with 10–20 measuring points each were performed across the filament. The ν_{15} (at 750 cm^{-1}) and the ν_{10} vibrational modes (at 1,637 cm^{-1}) were used as measure of cytochrome redox state, and data reported for each filament position are means of the quality-filtered and normalized band intensities (see *Data Analysis* in *SI Methods*). Statistical analyses are described in *SI Methods*.

Manipulation Experiments. Two manipulation experiments were performed where electron transport was inhibited and the change in cytochrome redox state was recorded by Raman microscopy. First, oxygen was removed from the oxic end of slide setup A by either filling the air inlet with nitrogen-flushed, oxygen-free water or by flushing it directly with a gentle flow of nitrogen gas. Raman spectra were recorded at approximately 500 μm from the sediment and at the midpoint between the sediment and the start of the oxic zone every 1–3 min over a period of 15–30 min before and after the manipulation. The first 5 min after removing oxygen were excluded to account for the time it took to fully deplete oxygen at the end of the cable bacteria. Oxygen was reintroduced by stopping the flow of nitrogen gas, and the response in cytochrome redox state was immediately recorded at midpoint only. Second, a laser microdissection microscope (Leica) was used to make two cuts 10 μm apart in the cable bacteria filament, approximately 1,000 μm from the sediment. Raman spectra were recorded at approximately 500 μm from the sediment, directly before and about 5 min after the cut. In both experiments, the band intensity at 750 cm^{-1} before the manipulation was normalized to 1, and any response to the manipulation is given as fold change relative to that value. Cable-bacteria filaments, which were only connected to the sediment but did not reach the oxic zone, were used as controls.

ACKNOWLEDGMENTS. We thank Lars B. Pedersen and Preben G. Sørensen for help with making the customized microsensors, Simon Agner Holm for providing the movie of cable bacteria, Anton Tramper, Silvia Hidalgo-Martinez, and Diana Vasquez-Cardenas for sediment collection, incubation, and transport, and Arno Schintlmeister and Bo Barker Jørgensen for valuable discussions. This study was supported by the European Research Council (Advanced Grant: Coulombus 291650), the Danish National Research Foundation (DNRF104 and DNRF136), and The Danish Council for Independent Research | Natural Sciences and Technology and Production Sciences. D.B. was supported in part by Austrian Science Fund (P26127-B20 and P27831-B28) and European Research Council (Starting Grant: FunKeyGut 741623). D.M. acknowledges the Netherlands Organisation for Scientific Research (NWO) Grant 722.011.003. P.T. was supported by the European Research Council under the European Union's Seventh Framework Program (FP7/20072013, European Research Council Grant 311341). F.J.R.M. was supported by the European Research Council (Grant: SedBioGeoChem 306933), the Research Foundation Flanders (FWO, Grant G031416N), and Vici Grant 016.VICI.170.072 from NWO. M.W. was supported by the European Research Council (Advanced Grant: NITRICARE 294343).

1. Pfeffer C, et al. (2012) Filamentous bacteria transport electrons over centimetre distances. *Nature* 491:218–221.
2. Malkin SY, et al. (2014) Natural occurrence of microbial sulphur oxidation by long-range electron transport in the seafloor. *ISME J* 8:1843–1854.
3. Risgaard-Petersen N, et al. (2015) Cable bacteria in freshwater sediments. *Appl Environ Microbiol* 81:6003–6011.
4. Trojan D, et al. (2016) A taxonomic framework for cable bacteria and proposal of the candidate genera Electrothrix and Electronema. *Syst Appl Microbiol* 39:297–306.
5. Burdorf LDW, et al. (2017) Long-distance electron transport occurs globally in marine sediments. *Biogeosciences* 14:683–701.
6. Nielsen LP, Risgaard-Petersen N, Fossing H, Christensen PB, Sayama M (2010) Electric currents couple spatially separated biogeochemical processes in marine sediment. *Nature* 463:1071–1074.
7. Meysman FJR, Risgaard-Petersen N, Malkin SY, Nielsen LP (2015) The geochemical fingerprint of microbial long-distance electron transport in the seafloor. *Geochim Cosmochim Acta* 152:122–142.
8. Lovley DR (2017) Syntrophy goes electric: Direct interspecies electron transfer. *Annu Rev Microbiol* 71:643–664.
9. Schauer R, et al. (2014) Succession of cable bacteria and electric currents in marine sediment. *ISME J* 8:1314–1322.
10. Risgaard-Petersen N, Revil A, Meister P, Nielsen LP (2012) Sulfur, iron-, and calcium cycling associated with natural electric currents running through marine sediment. *Geochim Cosmochim Acta* 92:1–13.
11. Meysman FJR (2017) Cable bacteria take a new breath using long-distance electricity. *Trends Microbiol* 26:411–422.

12. Esteve-Núñez A, Sosnik J, Visconti P, Lovley DR (2008) Fluorescent properties of c-type cytochromes reveal their potential role as an extracytoplasmic electron sink in Geobacter sulfurreducens. *Environ Microbiol* 10:497–505.
13. Virdis B, Harnisch F, Batstone DJ, Rabaey K, Donose BC (2012) Non-invasive characterization of electrochemically active microbial biofilms using confocal Raman microscopy. *Energy Environ Sci* 5:7017–7024.
14. Lebedev N, Strycharz-Glaven SM, Tender LM (2014) Spatially resolved confocal resonant Raman microscopic analysis of anode-grown Geobacter sulfurreducens biofilms. *ChemPhysChem* 15:320–327.
15. Robuschi L, Tomba JP, Busalmen JP (2017) Proving Geobacter biofilm connectivity with confocal Raman microscopy. *J Electroanal Chem (Lausanne Switz)* 793: 99–103.
16. Snider RM, Strycharz-Glaven SM, Tsoi SD, Erickson JS, Tender LM (2012) Long-range electron transport in Geobacter sulfurreducens biofilms is redox gradient-driven. *Proc Natl Acad Sci USA* 109:15467–15472.
17. Bjerg JT, Damgaard LR, Holm SA, Schramm A, Nielsen LP (2016) Motility of electric cable bacteria. *Appl Environ Microbiol* 82:3816–3821.
18. Oellerich S, Wackerbarth H, Hildebrandt P (2002) Spectroscopic characterisation of nonnative conformational states of cytochrome c. *J Phys Chem B* 106:6566–6580.
19. Kranich A, Ly HK, Hildebrandt P, Murgida DH (2008) Direct observation of the gating step in protein electron transfer: Electric-field-controlled protein dynamics. *J Am Chem Soc* 130:9844–9848.
20. Robuschi L, et al. (2013) Spectroscopic slicing to reveal internal redox gradients in electricity-producing biofilms. *Angew Chem Int Ed Engl* 52:925–928.
21. Brazhe NA, et al. (2012) Mapping of redox state of mitochondrial cytochromes in live cardiomyocytes using Raman microspectroscopy. *PLoS One* 7:e41990.
22. Adar F (1978) Resonance Raman spectra of ferric cytochrome c. A probe of low-lying electronic levels of the iron ion. *J Phys Chem* 82:230–234.
23. Strycharz-Glaven SM, Snider RM, Guiseppi-Elie A, Tender LM (2011) On the electrical conductivity of microbial nanowires and biofilms. *Energy Environ Sci* 4:4366–4379.
24. Steidl RJ, Lampa-Pastirk S, Reguera G (2016) Mechanistic stratification in electroactive biofilms of Geobacter sulfurreducens mediated by pilus nanowires. *Nat Commun* 7: 12217.